

STOCHASTIC NATURE OF GRAVITATIONAL WAVES FROM SUPERNOVA EXPLOSIONS WITH
STANDING ACCRETION SHOCK INSTABILITYKEI KOTAKE¹, WAKANA IWAKAMI², NAOFUMI OHNISHI², AND SHOICHI YAMADA^{3,4}

ABSTRACT

We study properties of gravitational waves based on the three-dimensional simulations, which demonstrate the neutrino-driven explosions aided by the standing accretion shock instability (SASI). Pushed by evidence supporting slow rotation prior to core-collapse, we focus on the asphericities in neutrino emissions and matter motions outside the protoneutron star. By performing a ray-tracing calculation in 3D, we estimate accurately the gravitational waveforms from anisotropic neutrino emissions. In contrast to the previous work assuming axisymmetry, we find that the gravitational waveforms vary much more stochastically because the explosion anisotropies depend sensitively on the growth of the SASI which develops chaotically in all directions. Our results show that the gravitational-wave spectrum has its peak near ~ 100 Hz, reflecting the SASI-induced matter overturns of $\sim O(10)$ ms. We point out that the detection of such signals, possibly visible to the LIGO-class detectors for a Galactic supernova, could be an important probe into the long-veiled explosion mechanism.

Subject headings: supernovae: general — gravitational waves — neutrinos — hydrodynamics — instability

1. INTRODUCTION

The gravitational-wave astronomy is now becoming reality. In fact, significant progress has been made on the gravitational wave detectors, such as LIGO, VIGRO, GEO600, TAMA300, and AIGO with their international network of the observatories (e.g., Hough & Rowan (2005) for a review). For the detectors, core-collapse supernovae especially in our Galaxy, have been supposed as one of the most plausible sources of gravitational waves (see, for example, Kotake et al. (2006); Ott (2009) for recent reviews).

Traditionally, most of the model calculations of gravitational waves (GWs) have focused on the bounce signals in the context of rotational (e.g., Zwerger & Müller (1997); Kotake et al. (2003); Shibata & Sekiguchi (2004); Ott et al. (2004); Dimmelfeier et al. (2007); Scheidegger et al. (2008) and references therein) and magnetrotational core-collapse (Kotake et al. 2004; Obergaulinger et al. 2006; Cerdá-Durán et al. 2007). However recent stellar evolution calculations suggest that such rapid rotation assumed in most of the previous studies, albeit attracting much attention currently as a relevance to collapsar (Hirschi et al. 2005; Woosley & Heger 2006), is not canonical for progenitors of core-collapse supernovae with neutron star formations (Heger et al. 2005; Ott et al. 2006)

In the case of the slowly rotating supernova cores, two other ingredients are expected to be important in the much later phases after core bounce, namely convective motions and anisotropic neutrino emissions. Thus far, various physical ingredients for producing asphericities

and the resulting GWs in the postbounce phase, have been studied such as the roles of pre-collapse density inhomogeneities (Burrows & Hayes 1996; Müller & Janka 1997; Fryer 2004), moderate rotation of the iron core (Müller et al. 2004), g-mode oscillations of protoneutron stars (PNSs) (Ott et al. 2006), and the standing-accretion-shock-instability (SASI) (Kotake et al. 2007; Marek et al. 2009).

However, most of them have been based on two-dimensional (2D) simulations that assume axisymmetry. Then, the growth of SASI (e.g., Blondin et al. (2003); Scheck et al. (2004); Ohnishi et al. (2006); Foglizzo et al. (2007)) and the large-scale convection, both of which are now considered to generically develop in the postbounce phase and to help the neutrino-driven explosions (Bethe 1990; Marek & Janka 2009), develop along the symmetry axis preferentially, thus suppressing the anisotropies in explosions. So far very few three-dimensional (3D) studies have been conducted (Müller & Janka 1997; Fryer et al. 2004). Moreover, neither the growth of the SASI nor its effects on the GWs have been studied yet because SASI is suppressed artificially owing to the limited computational domain (Müller & Janka 1997) or to the early shock-revival (Fryer et al. 2004), which has not been discovered by other supernova simulations.

In this *Letter*, we study the properties of the gravitational radiation based on the 3D simulations, which demonstrate the neutrino-driven explosions aided by SASI (Iwakami et al. 2008a). Supported by the evidence of the slow rotation prior to core-collapse (Heger et al. 2005; Ott et al. 2006), we focus on the asphericities outside the protoneutron stars, which are produced by the growth of SASI. By performing a ray-tracing calculation in 3D (Kotake et al. 2009), we estimate accurately the gravitational waveforms from anisotropic neutrino emissions. We show that the features of the gravitational waveforms are significantly different than the ones in the axisymmetric cases, which should tell us the necessity of the 3D supernova modeling.

¹ Division of Theoretical Astronomy/Center for Computational Astrophysics, National Astronomical Observatory of Japan, 2-21-1, Osawa, Mitaka, Tokyo, 181-8588, Japan

² Department of Aerospace Engineering, Tohoku University, 6-6-01 Aramaki-Aza-Aoba, Aoba-ku, Sendai, 980-8579, Japan

³ Science & Engineering, Waseda University, 3-4-1 Okubo, Shinjuku, Tokyo, 169-8555, Japan

⁴ Advanced Research Institute for Science and Engineering, Waseda University, 3-4-1 Okubo, Shinjuku, Tokyo, 169-8555, Japan

2. NUMERICAL METHODS AND MODELS

The employed numerical methods and model concepts are essentially the same as those in our previous paper (Iwakami et al. 2008a). Using the ZEUS-MP (Hayes et al. 2006) as a hydro-solver, we solve the dynamics of the standing accretion shock flows of matter attracted by the protoneutron star and irradiated by neutrinos emitted from the protoneutron star. We employ the so-called light-bulb approximation (see, e.g., Janka & Müller (1996)) and adjust the neutrino luminosities from the PNSs to trigger explosions.

The computational grid is comprised of 300 logarithmically spaced, radial zones to cover from the absorbing inner boundary of ~ 50 km to the outer boundary of 2000 km, and 30 polar (θ) and 60 azimuthal (ϕ) uniform mesh points, which are used to cover the whole solid angle (see for the resolution tests in Iwakami et al. (2008a)).

The initial conditions are provided in the same manner of Ohnishi et al. (2006), which describes the spherically symmetric steady accretion flow through a standing shock wave (Yamasaki & Yamada 2005). To induce non-spherical instability we add random velocity perturbations to be less than 1 % of the unperturbed velocity. Changing the input (electron-)neutrino luminosity at the surface of the protoneutron star from $L_\nu = 6.4 - 6.85 \times 10^{52}$ erg s $^{-1}$, we have computed six 3D models and one 2D model (see Table 1.) Except for model E, we can observe the continuous increase of the average shock radius with the growth of SASI, reaching the outer boundary of the computational domain with the explosion energy of $\sim 10^{51}$ erg. Until this moment, we run the simulations (e.g., Δt in the table).

Following the method in Epstein (1978); Müller & Janka (1997), the two modes of the GWs from anisotropic neutrino emissions are derived as follows,

$$h_+ = C \int_0^t \int_{4\pi} d\Omega' (1 + s(\theta')c(\phi')s(\xi) + c(\theta')c(\xi)) \times \frac{(s(\theta')c(\phi')c(\xi) - c(\theta')s(\xi))^2 - s^2(\theta')s^2(\phi')}{[s(\theta')c(\phi')c(\xi) - c(\theta')s(\xi)]^2 + s^2(\theta')s^2(\phi')} \frac{dl_\nu(\Omega', t')}{d\Omega'}$$

and

$$h_\times = 2C \int_0^t \int_{4\pi} d\Omega' (1 + s(\theta')c(\phi')s(\xi) + c(\theta')c(\xi)) \times \frac{s(\theta')s(\phi')(s(\theta')c(\phi')c(\xi) - c(\theta')s(\xi))}{[s(\theta')c(\phi')c(\xi) - c(\theta')s(\xi)]^2 + s^2(\theta')s^2(\phi')} \frac{dl_\nu(\Omega', t')}{d\Omega'}$$

where $s(A) \equiv \sin(A)$, $c(B) \equiv \cos B$, $C \equiv 2G/(c^4 R)$ with G , c and R , being the gravitational constant, the speed of light, the distance of the source to the observer respectively, $dl_\nu/d\Omega$ represents the direction-dependent neutrino luminosity emitted per unit of solid angle into direction of Ω , and ξ is the viewing angle (e.g., Kotake et al. (2009)). For simplicity, we consider here two cases, in which the observer is assumed to be situated along 'polar' ($\xi = 0$) or 'equatorial' ($\xi = \pi/2$) direction. To determine $dl_\nu/d\Omega$, we perform a ray-tracing calculation. Since the regions outside the PNSs are basically thin to neutrinos, we solve the neutrino transport equations in a post-processing manner to estimate the neutrino anisotropy, in which neutrino absorptions and emissions

TABLE 1
MODEL SUMMARY

Model	L_ν (10^{52} erg/s)	Δt (ms)	$ h_{\max}^p $ (10^{-22})	$ h_{\max}^e $ (10^{-22})	E_{GW} ($10^{-11} M_\odot c^2$)
A	6.8	507	3.0(\times)	3.1(\times)	6.0
B	6.766	512	2.4(+)	3.1(\times)	7.4
C	6.7	532	3.7(\times)	2.6(\times)	7.4
D	6.6	667	2.0(\times)	2.0(+)	10.8
E	6.4	—	0.7(+)	1.6(\times)	2.6
F	6.85	429	2.1(\times)	4.3(+)	5.6
A'(2D)	6.8	509	—	7.7(+)	4.4

NOTE. — L_ν denotes the input luminosity. Δt represents the simulation time. Model A' is the 2D version of model A. $|h_{\max}^p|$ and $|h_{\max}^e|$ represents the maximum amplitudes seen from the pole or the equator, respectively. + or \times indicates the polarization of the GWs at the maximum. E_{GW} is the total radiated GW energy. The supernova is assumed to be located at a distance of 10 kpc.

by free nucleons, dominant outside the PNSs, are taken into account (see Kotake et al. (2009) for more details). To get the numerical convergence, we need to set 45000 rays to determine the luminosity for each given direction of Ω . The GW amplitudes from mass motions are extracted by using the standard quadrupole formula (e.g., Müller & Janka (1997)), and their spectra by Flanagan & Hughes (1998) with the FFT techniques.

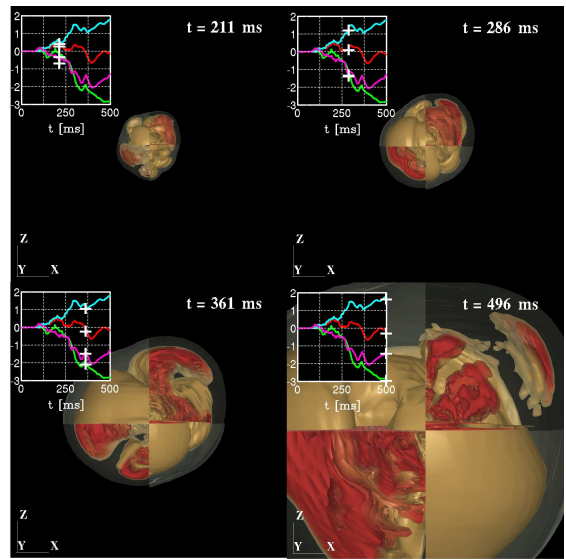


FIG. 1.— Four snapshots of the entropy distributions of model A. The second and fourth quadrant of each panel shows the surface of the standing shock wave. In the first and third quadrant, the profiles of the high entropy bubbles (colored by red) inside the section cut by the ZX plane are shown. The side length of each plot is 1000km. The insets show the gravitational waveforms from anisotropic neutrino emissions, with '+' on each curves representing the time of the snapshot. Note that the colors of the curves are taken to be the same as the top panel of Figure 2.

3. RESULTS

Figure 1 shows the 3D hydrodynamics features of SASI from the early phase of the non-linear regime of SASI (top left) until the shock break-out (bottom right) with the gravitational waveform from neutrinos inserted in each panel.

After about 100 ms, the deformation of the standing

shock becomes remarkable marking the epoch when the SASI enters the non-linear regime (top left of Figure 1). At the same time, the gravitational amplitudes begin to deviate from zero. Comparing the top two panels in Figure 2, which shows the total amplitudes (top) and the neutrino contribution only (bottom), it can be seen that the gross structures of the waveforms are predominantly determined by the neutrino-originated GWs with the slower temporal variations ($\gtrsim 30 - 50$ ms), to which the GWs from matter motions with rapid temporal variations ($\lesssim 10$ ms) are superimposed. So, we first pay attention to the neutrino GWs in the following and discuss the importance of the matter GWs later in the spectrum analysis.

As seen from the top right through bottom left to right panels of Figure 1, the major axis of the growth of SASI is shown to be not aligned with the symmetric axis (:Z axis in the figure) and the flow inside the standing shock wave is not symmetric with respect to this major axis (see the first and third quadrant in Figure 1). This is a generic feature in the computed 3D models, which is in contrast to the axisymmetric case. The GW amplitudes from SASI in 2D showed an increasing trend with time due to the symmetry axis, along which SASI can develop preferentially (Kotake et al. 2007, 2009). Free from such a restriction, a variety of the waveforms is shown to appear (see waveforms inserted in Figure 1). Furthermore, the 3D standing shock can also oscillate in all directions, which leads to the smaller explosion anisotropy than 2D. With these two factors, the maximum amplitudes seen either from the equator or the pole becomes smaller than 2D (compare $|h_{\max}^e|$ in Table 1 for models A and A'). On the other hand, their sum in terms of the total radiated energy (E_{GW} in Table 1) are found to be almost comparable between 2D and 3D models, which is likely to imply the energy equipartition with respect to the spatial dimensions. It was reported in a pioneering 3D study (Müller & Janka 1997) that the emitted GW energy in the forms of neutrinos was reported to be about 2 orders of magnitude smaller for 3D than in 2D. However this may be because the global anisotropy of the SASI was not captured in their simulations with the limited computation domain in the polar direction.

Figure 2 shows the gravitational waveforms for different luminosity models. The input luminosity for the two pair panels differs only 0.5%. Despite the slight difference, the waveforms of each polarization are shown to exhibit no systematic similarity when seen from the pole or equator. This is due to the chaotic nature of SASI influenced by small differences. No systematic dependence of the maximum amplitudes and the radiated GW energies on the neutrino luminosities is found among the models investigated here (see Table 1). In fact, the largest emitted GW energy is obtained for model D with the intermediate neutrino luminosity (Table 1). It is noted that the waveforms are even sensitive to the difference of the grid zoning due to the stochastic nature, although no significant difference in the GW amplitudes is seen in the numerical run with twice as many grid points in the θ and ϕ directions.

Now we move on to discuss the features of the waveforms by the spectrum analysis. From Figure 3, it can be seen that the neutrino GWs, albeit dominant over the matter GWs in the lower frequencies below ~ 10 Hz, be-

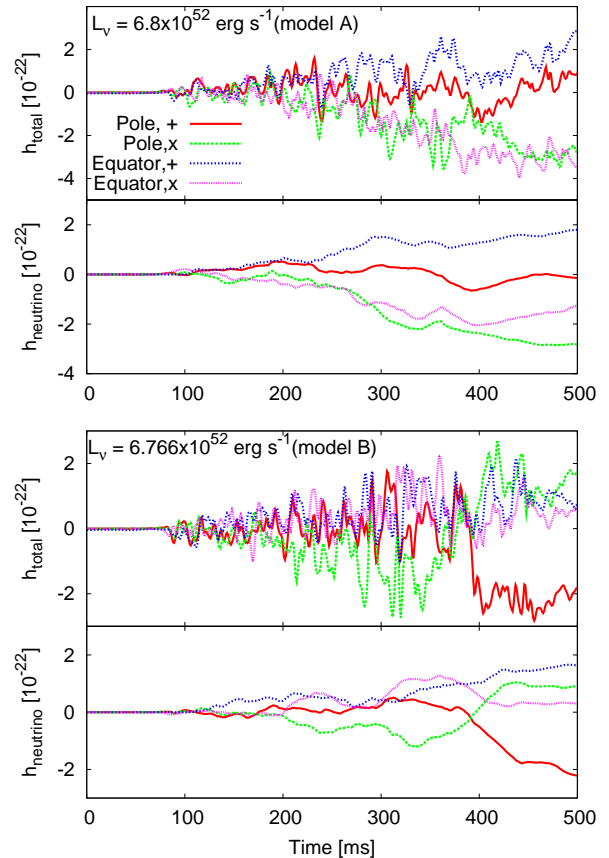


FIG. 2.— Gravitational waveforms from neutrinos (bottom) and from the sum of neutrinos and matter motions (top), seen from the polar axis and along the equator (indicated by 'Pole' and 'Equator') with polarization (+ or \times modes) for models A and B. The distance to the SN is assumed to be 10 kpc.

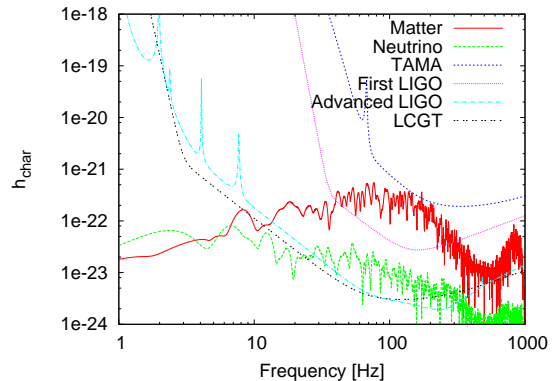


FIG. 3.— Characteristic gravitational-wave spectra from anisotropic neutrino emissions ('Neutrino') and matter motions ('Matter') with optimal detection limits of TAMA, the first LIGO, advanced LIGO, and LCGT for a supernova at a distance of 10 kpc.

come very difficult to detect for ground-based detectors whose sensitivity is limited mainly by the seismic noises at such lower frequencies (Ando et al. 2005; Abbott et al. 2005; Weinstein 2002; Kuroda et al. 1999). On the other hand, the gravitational-wave spectra from matter motions peak near ~ 100 Hz, reflecting the growth of $\ell = 2$ mode of SASI with timescales of $O(10)$ ms. Such sig-

nals from a Galactic supernova are probably within the detection limits of the LIGO-class detectors, and seem surely visible to the next-generation detectors such as the advanced LIGO and LCGT. It is noted that another peak in the GW spectra near ~ 1 kHz is from the rapidly varying matter motions of $O(\text{ms})$, induced by the local hydrodynamical instabilities. These gross properties in the GW spectra are found to be common to the other luminosity models. Thus the peak in the spectra near ~ 100 Hz is a characteristic feature obtained in the 3D models computed here.

4. SUMMARY AND DISCUSSION

We studied the properties of GWs based on the 3D simulations, which demonstrate the neutrino-driven explosions with SASI. We focused on the asphericities outside the protoneutron stars, which are produced by the growth of SASI. By performing a ray-tracing calculation in 3D, we estimated accurately the gravitational waveforms from anisotropic neutrino emissions. Our results showed that the waveforms vary much more stochastically than for 2D because the explosion anisotropies depend sensitively on the growth of the SASI which develops chaotically in all directions. From the spectra analysis, it was pointed out that the gravitational-wave spectra from matter motions peak near ~ 100 Hz, reflecting the growth of $\ell = 2$ mode of SASI, and that such signals are probably visible to LIGO-class detectors for a Galactic source.

Here it should be noted that the simulations highlighted in this paper are only a very first step towards realistic 3D modeling of the supernova explosions. The approximations adopted in this paper, such as the replacement of the PNS by the fixed inner boundary and the light-bulb approach with the constant neutrino luminosity, should be improved. Important ingredients for

the GW emissions such as the oscillations of the PNSs (Burrows et al. 2006) and the enhanced neutrino emissions near the equators deep inside the PNS observed in Marek et al. (2009), cannot be treated in principle here. The exploration of these phenomena will require consistent simulations covering the entire stellar core and starting from gravitational collapse with neutrino transfer coupled to the 3D magnetohydrodynamics. Besides, the effects of rotation on the SASI are yet to be investigated (Iwakami et al. 2008b), although the construction of the rotating steady accretion flows is still a major undertaking.

Bearing these caveats in mind, the stochastic nature of the GWs, which is illuminated here by the 3D models, is qualitatively new. It should be also mentioned that the GW spectra for the acoustic mechanism showed a very strong peak near \sim kHz, reflecting the g-modes oscillations of the PNS (Ott et al. 2006), and are significantly different from the waveforms discussed here for the SASI-aided neutrino-driven models. This means that the successful detection of the GW signals will supply us a powerful tool to probe the explosion mechanism. Recently the next-generation detectors, by which the GWs studied here could be surely visible for a Galactic source, are planned to be on line soon (2014!) (Lantz 2006). Here it is an urgent task for theorists to make precise predictions of the GW signals based on more sophisticated 3D supernova modeling.

KK would like to thank K. Sato for continuing encouragements. KK and SY are grateful to H.-Th. Janka and E. Müller for their kind hospitality during their stay in MPA. Numerical computations were carried on XT4 at CfCA of the NAOJ. This study was supported in part by the Grants-in-Aid for the Scientific Research from the Ministry of Education, Science and Culture of Japan (Nos. 19540309 and 20740150).

REFERENCES

- Ando, M., et al. 2005, *Classical and Quantum Gravity*, 22, 1283
 Abbott, B., et al. 2005, *Phys. Rev. D*, 72, 122004
 Bethe, H. A. 1990, *Reviews of Modern Physics*, 62, 801
 Blondin, J. M., Mezzacappa, A., & DeMarino, C. 2003, *ApJ*, 584, 971
 Burrows, A. & Hayes, J. 1996, *Physical Review Letters*, 76, 352
 Burrows, A., Livne, E., Dessart, L., Ott, C. D., & Murphy, J. 2006, *ApJ*, 640, 878
 Cerdá-Durán, P., Font, J. A., & Dimmelmeier, H. 2007, *A&A*, 474, 169
 Dimmelmeier, H., Ott, C. D., Janka, H.-T., Marek, A., Müller, E. 2007, *Physical Review Letters*, 98, 251101
 Epstein, R. 1978, *ApJ*, 223, 1037
 Flanagan, É. É., & Hughes, S. A. 1998, *Phys. Rev. D*, 57, 4566
 Foglizzo, T., Galletti, P., Scheck, L., & Janka, H.-T. 2007, *ApJ*, 654, 1006
 Fryer, C. L., Holz, D. E., & Hughes, S. A. 2004, *ApJ*, 609, 288
 Fryer, C. L. 2004, *ApJ*, 601, L175
 Hayes, J. C., Norman, M. L., Fiedler, R. A., Bordner, J. O., Li, P. S., et al. 2006, *ApJS*, 165, 188
 Heger, A., Woosley, S. E., & Spruit, H. C. 2005, *ApJ*, 626, 350
 Hirschi, R., Meynet, G., & Maeder, A. 2005, *A&A*, 443, 581
 Hough, J., & Rowan, S. 2005, *Journal of Optics A: Pure and Applied Optics*, 7, 257
 Iwakami, W., Kotake, K., Ohnishi, N., Yamada, S., & Sawada, K. 2008, *ApJ*, 678, 1207
 Iwakami, W., Kotake, K., Ohnishi, N., Yamada, S., & Sawada, K. 2008, arXiv:0811.0651
 Janka, H.-T., & Müller, E. 1996, *A&A*, 306, 167
 Kotake, K., Yamada, S., & Sato, K. 2003, *Phys. Rev. D*, 68, 044023
 Kotake, K., Yamada, S., Sato, K., Sumiyoshi, K., Ono, H., & Suzuki, H. 2004, *Phys. Rev. D*, 69, 124004
 Kotake, K., Sato, K., & Takahashi, K. 2006, *Reports of Progress in Physics*, 69, 971
 Kotake, K., Ohnishi, N., & Yamada, S. 2007, *ApJ*, 655, 406
 Kotake, K., Iwakami, W., Ohnishi, N., & Yamada, S. 2009, submitted to *ApJ*
 Kuroda, K and LCGT Collaboration, *Int. J. Mod. Phys. D*, 5, 557, (1999).
 Lantz, B. 2006, APS Meeting Abstracts, <http://www.ligo.caltech.edu/advLIGO/>
 Marek, A., & Janka, H.-T. 2009, *ApJ*, 694, 664
 Marek, A., Janka, H.-T., Müller, E. 2009, *A&A*, 496, 475
 Müller, E., Rampp, M., Buras, R., Janka, H.-T., & Shoemaker, D. H. 2004, *ApJ*, 603, 221
 Müller, E., & Janka, H.-T. 1997, *A&A*, 317, 140
 Obergaulinger, M., Aloy, M. A., Müller, E. 2006, *A&A*, 450, 1107
 Ohnishi, N., Kotake, K., & Yamada, S. 2006, *ApJ*, 641, 1018
 Ott, C. D., Burrows, A., Livne, E., & Walder, R. 2004, *ApJ*, 600, 834
 Ott, C. D., Burrows, A., Thompson, T. A., Livne, E., & Walder, R. 2006, *ApJS*, 164, 130
 Ott, C. D., Burrows, A., Dessart, L., & Livne, E. 2006, *Physical Review Letters*, 96, 201102
 Ott, C. D. 2009, *Classical and Quantum Gravity*, 26, 063001
 Scheck, L., Plewa, T., Janka, H.-T., Kifonidis, K., Müller, E. 2004, *Physical Review Letters*, 92, 011103
 Scheidegger, S., Fischer, T., Whitehouse, S. C., & Liebendörfer, M. 2008, *A&A*, 490, 231
 Shibata, M., & Sekiguchi, Y. 2004, *Phys. Rev. D*, 69, 084024
 Weinstein, A. 2002, *Classical and Quantum Gravity*, 19, 1575

Woosley, S. E., & Heger, A. 2006, ApJ, 637, 914
Yamasaki, T., & Yamada, S. 2005, ApJ, 623, 1000
Zwergner, T., & Mueller, E. 1997, A&A, 320, 209